# Amorphous ZnO and Oxygen Vacancies Modified Nitrogen-Doped Carbon Skeleton with Lithiophilicity and Ionic Conductivity for Stable Lithium Metal Anode

Fei Wang[a], Jingxia Gao[b],Yong Liu[a,c,*], Fengzhang Ren[a,*],

[a] School of Materials Science and Engineering, Henan University of Science and Technology, Provincial and Ministerial Co-construction of Collaborative Innovation Center for Non-ferrous Metal new Materials and Advanced Processing Technology, Luoyang 471023, China

[b] Faculty of engineering, Huanghe Science and Technology College, Zhengzhou, Henan 450006, China

[c] Henan Key Laboratory of Non-Ferrous Materials Science & Processing Technology, Luoyang 471023, China

* Corresponding author and E-mail address:

Prof. Yong Liu, liuyong209@haust.edu.cn;

Prof. Fengzhang Ren, renfz@haust.edu.cn;

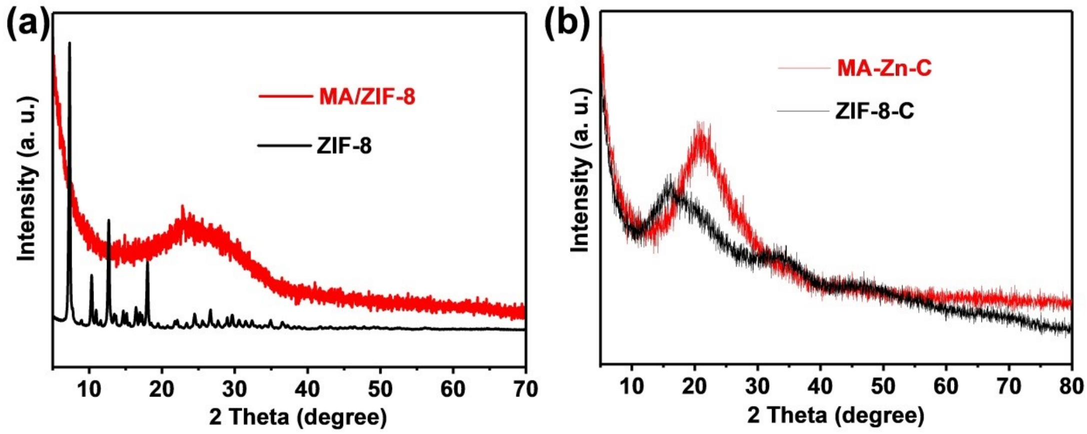


Figure S1. XRD patterns of (a) ZIF-8 and MA/ZIF-8, and (b) ZIF-8-C and MA-Zn-C.

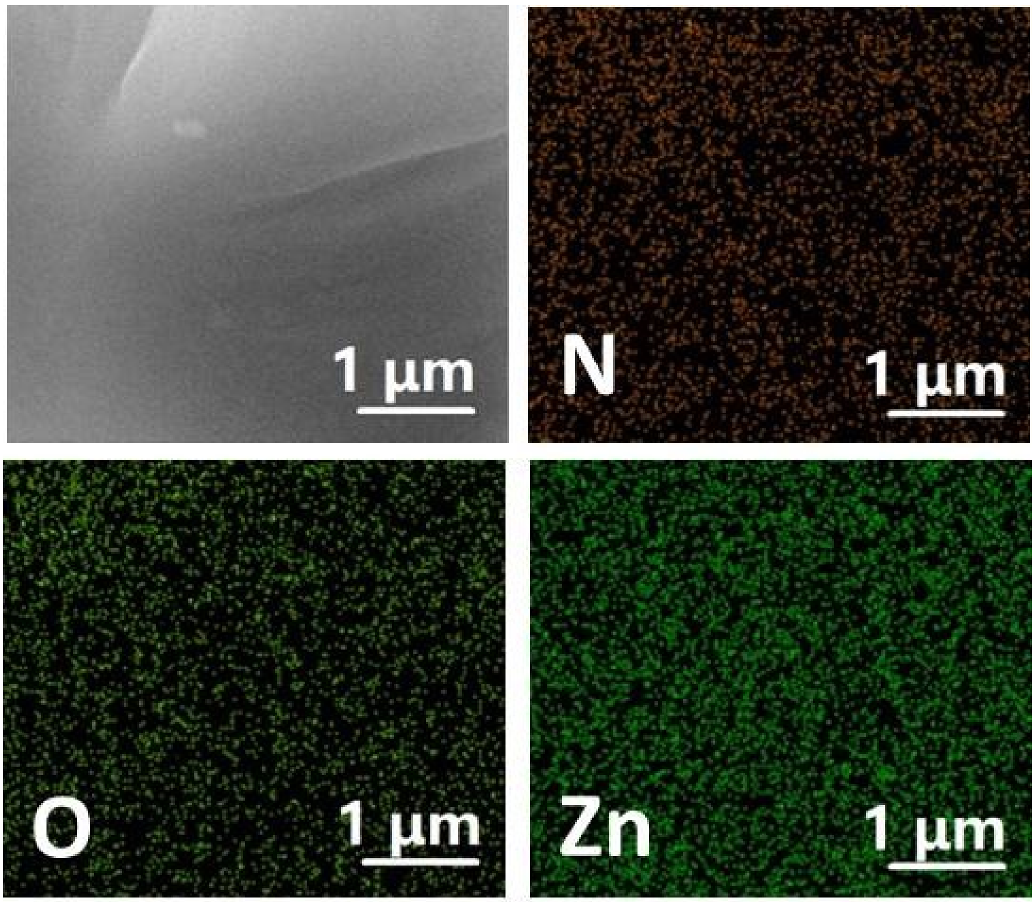


Figure S2. SEM images of MA-Zn-C, and the corresponding elemental mapping.

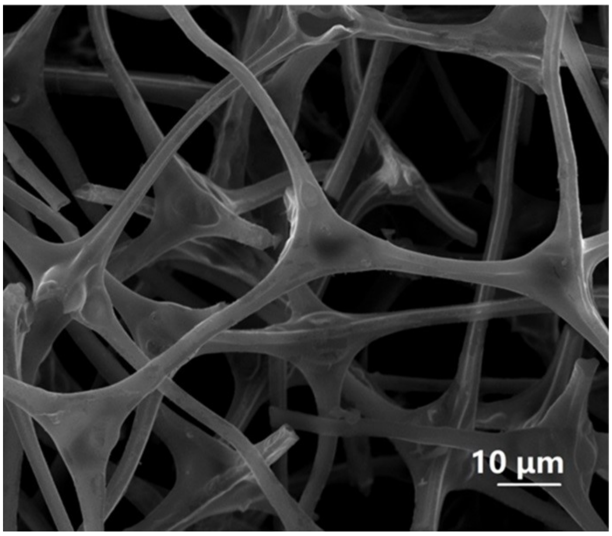


Figure S3. SEM image of MA-C.

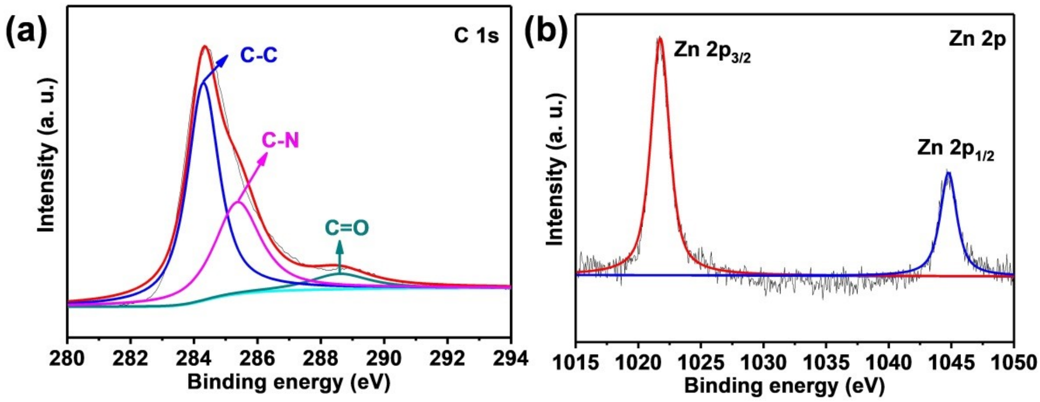


Figure S4. (a) C 1s and (b) Zn 2p XPS spectra of MA-Zn-C.

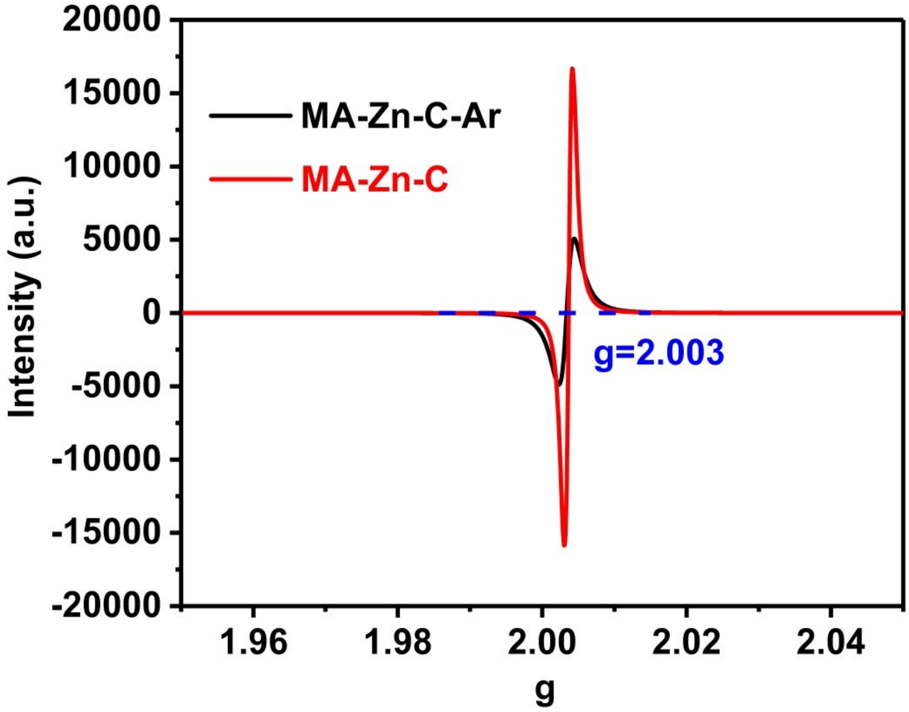


Figure S5. ESR spectra of prepared MA-Zn-C-Ar and MA-Zn-C.

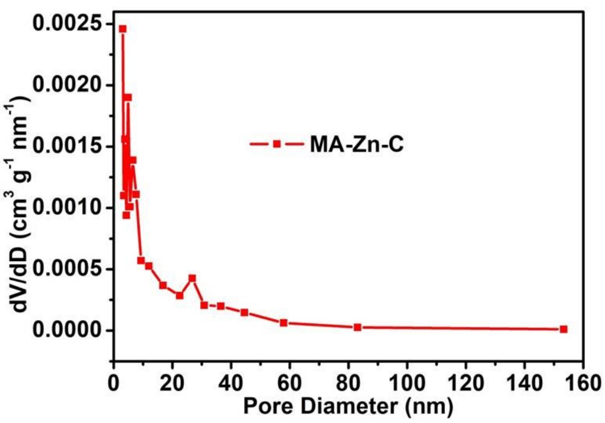


Figure S6. The pore size distribution curve of MA-Zn-C.

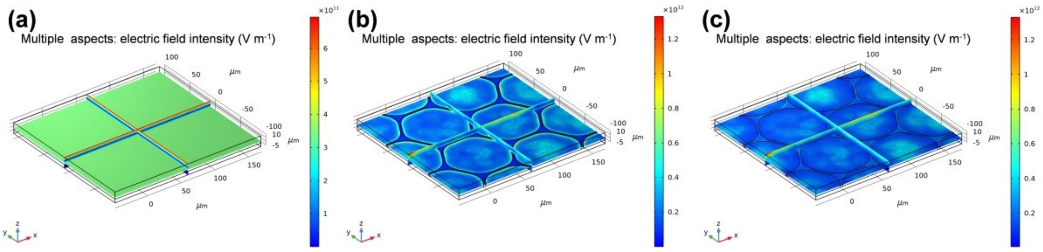


Figure S7. Electric field intensity distribution diagrams of (a) Cu foil, (b) MA-C, and (c) MA-Zn-C.

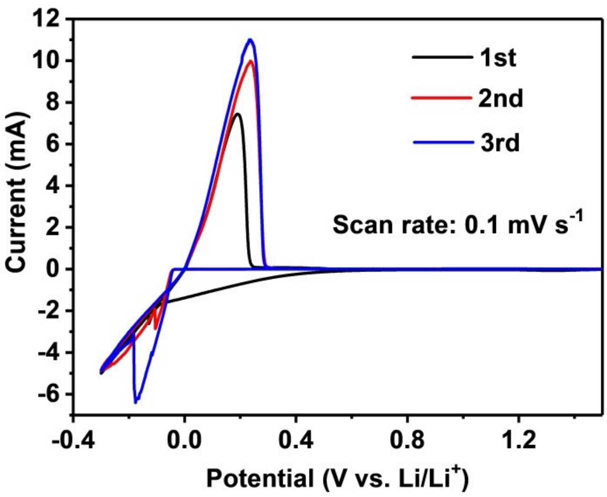


Figure S8. Cyclic voltammetry curves of MA-Zn-C at the scan rate of 0.1 mV $s^{-1}$.

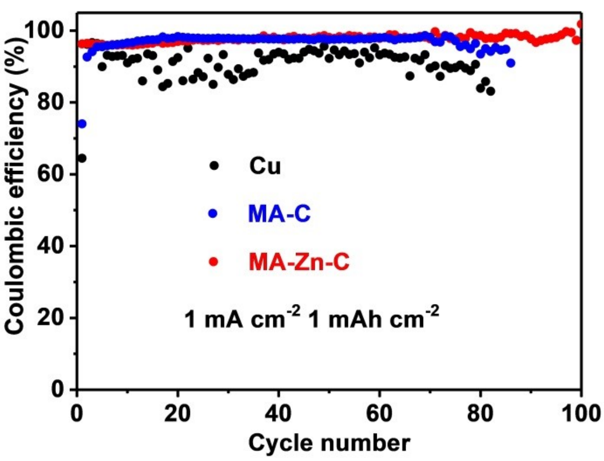


Figure S9. CE of Cu, MA-C and MA-Zn-C electrode with lithium deposition amount of 1 mAh $cm^{-2}$ at 1 mA $cm^{-2}$.

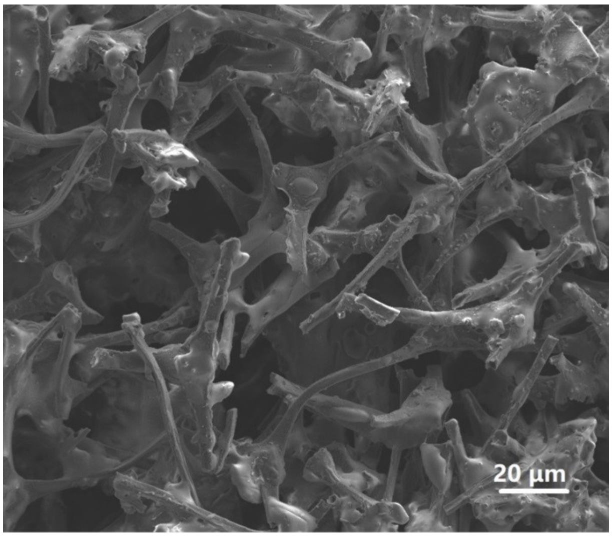


Figure S10. SEM image of MA-Zn-C-Li after Li stripping.

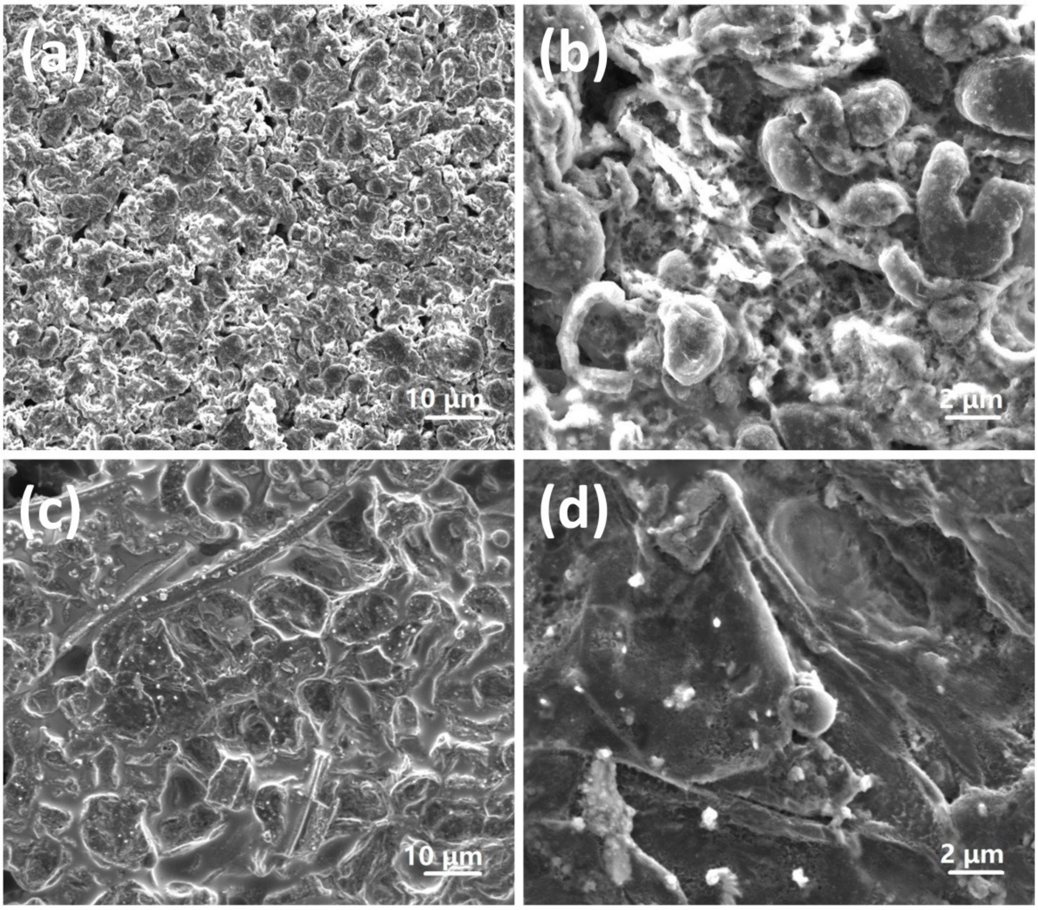


Figure S11. SEM images of (a,b) MA-C and (c,d) MA-Zn-C electrode after cycles at 1 mA cm$^{-2}$-1 mAh cm$^{-2}$.

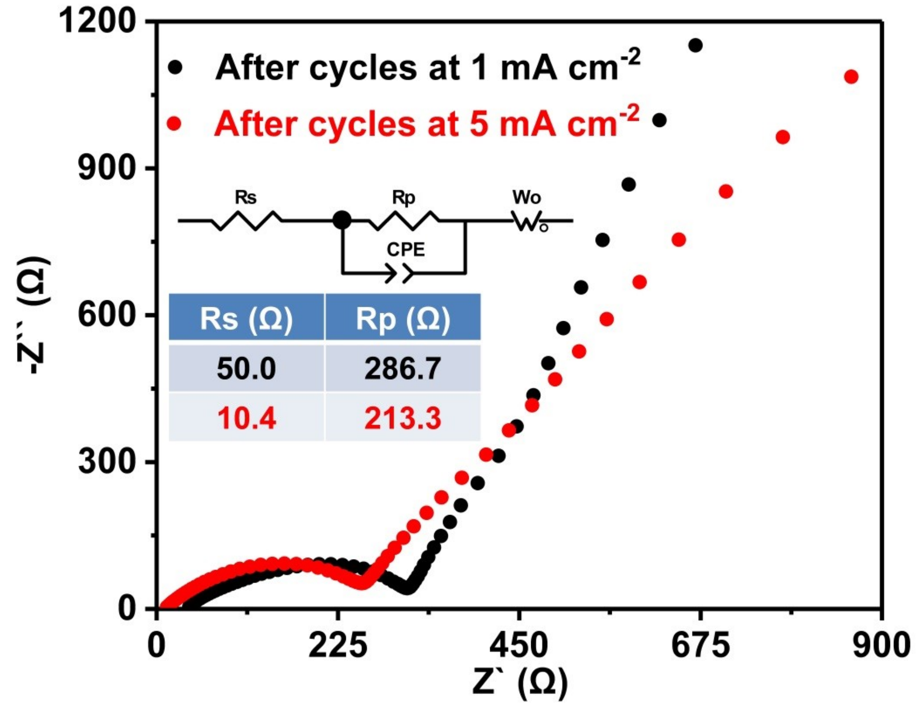


Figure S12. Nyquist plots of the MA-Zn-C-Li//MA-Zn-C-Li cells after cycles at 1 mA cm$^{-2}$ and 5 mA cm$^{-2}$.

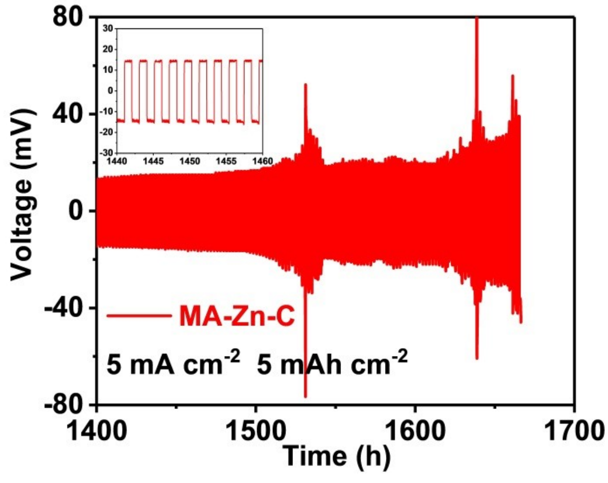


Figure S13. Consecutive cyclic performance of MA-Zn-C-Li//MA-Zn-C-Li symmetrical cell at 5 mA cm$^{-2}$-5 mAh cm$^{-2}$.

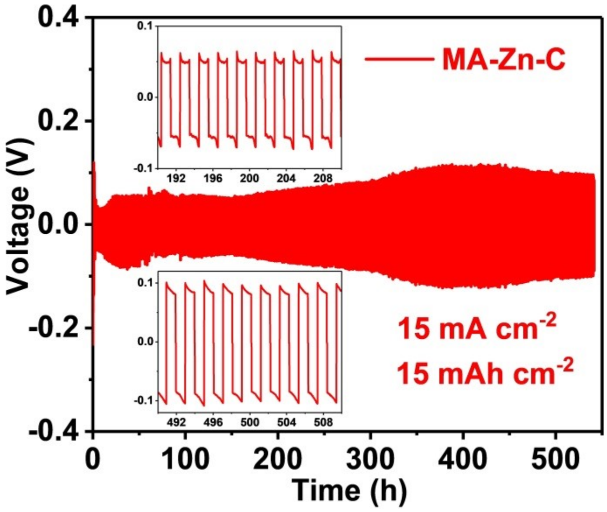


Figure S14. Cyclic performance of MA-Zn-C-Li//MA-Zn-C-Li symmetrical cell at 15 mA $cm^{-2}$-15 mAh $cm^{-2}$.

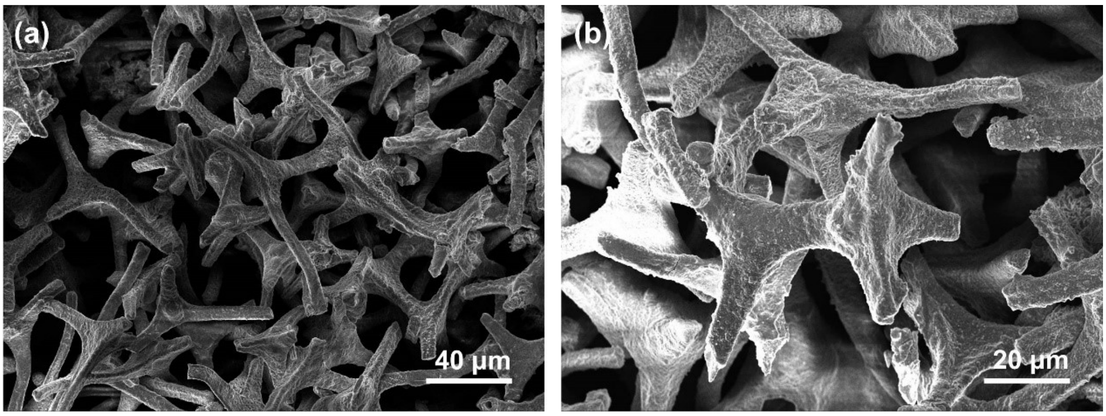


Figure S15. The SEM image of MA-Zn-C-Li after Li stripping.

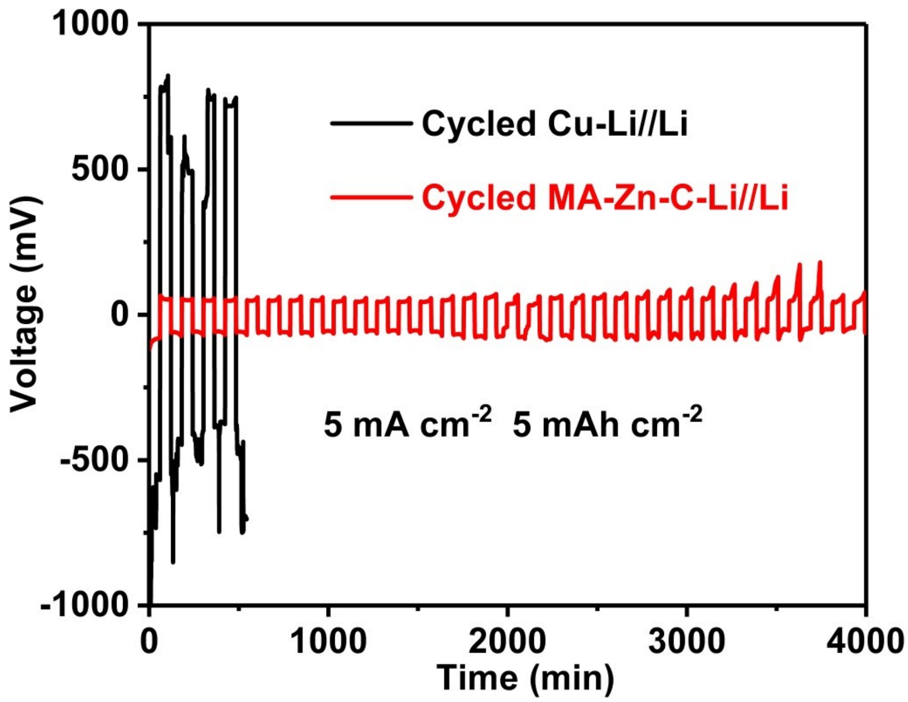


Figure S16. Electrochemical performances of cycled Cu-Li/Li and cycled MA-Zn-C-Li/Li at 5 mA cm$^{-2}$ and 5 mAh cm$^{-2}$ after long cycles.

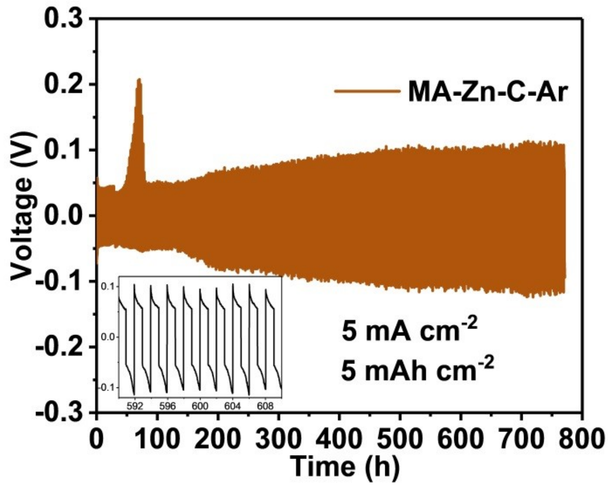


Figure S17. Cyclic performance of MA-Zn-C-Ar-Li//MA-Zn-C-Ar-Li symmetrical cell at 5 mA cm$^{-2}$-5 mAh cm$^{-2}$.

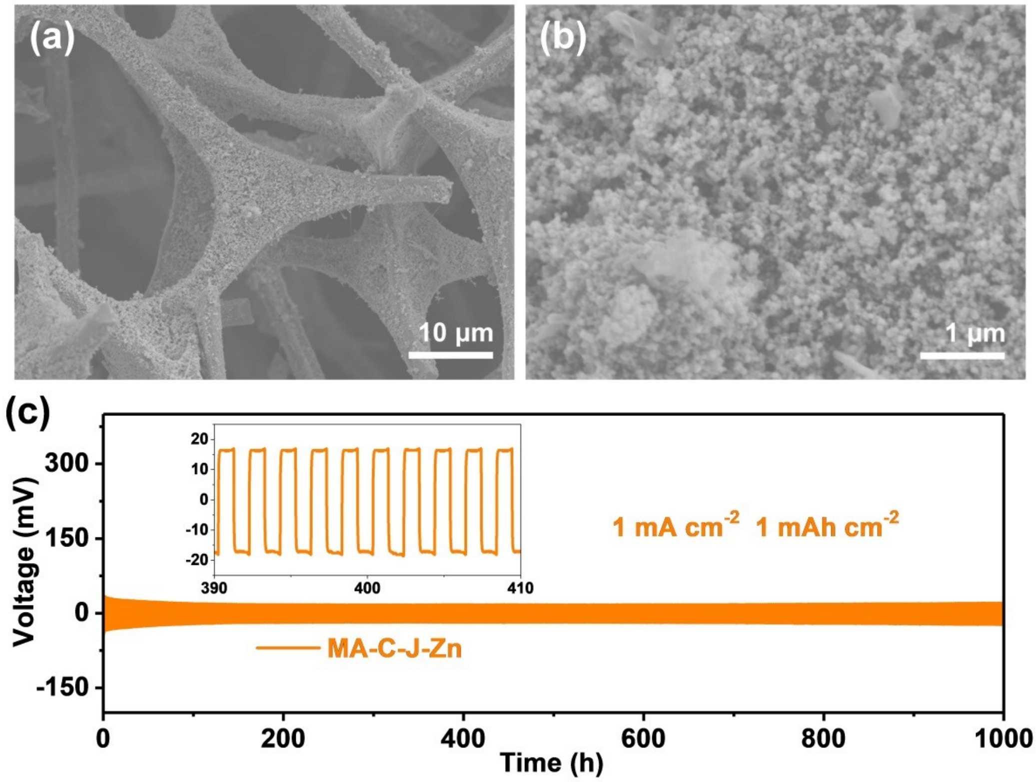


Figure S18. Cyclic performance of MA-C-J-Zn-Li// MA-C-J-Zn-Li symmetrical cell at 1 mA $cm^{-2}$-1 mAh $cm^{-2}$.

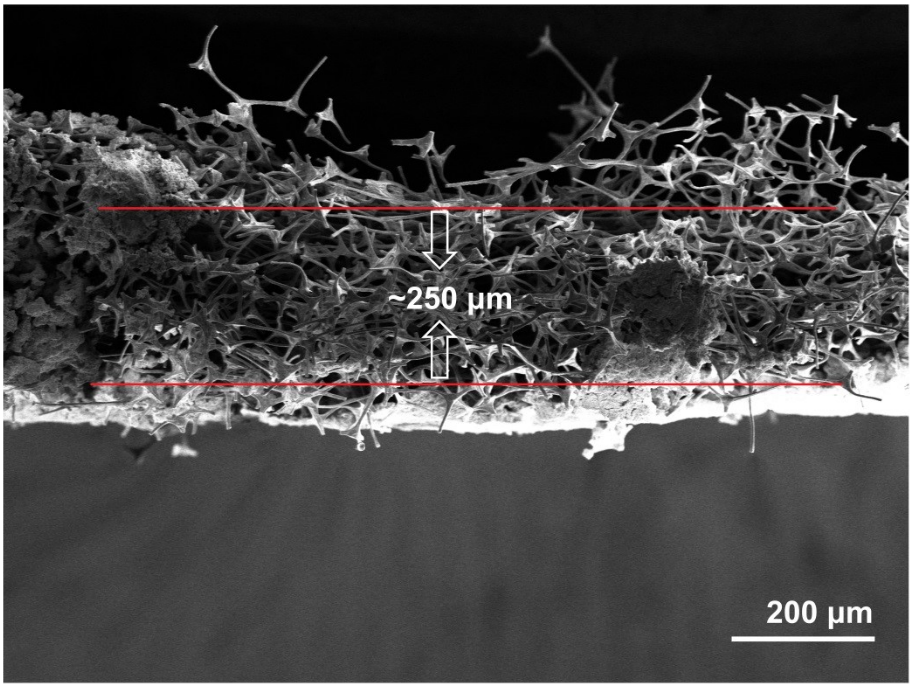


Figure S19. The sectional view of MA-Zn-C-Li composite used as the composite anode in full cells.

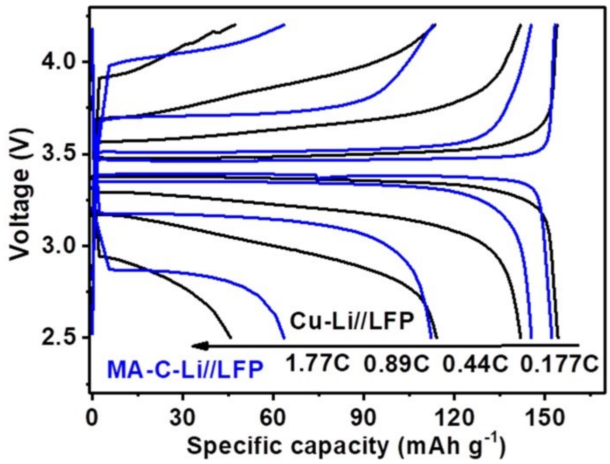


Figure S20. Charge/discharge curves of Cu-Li//LFP and MA-C-Li//LFP at various current densities.

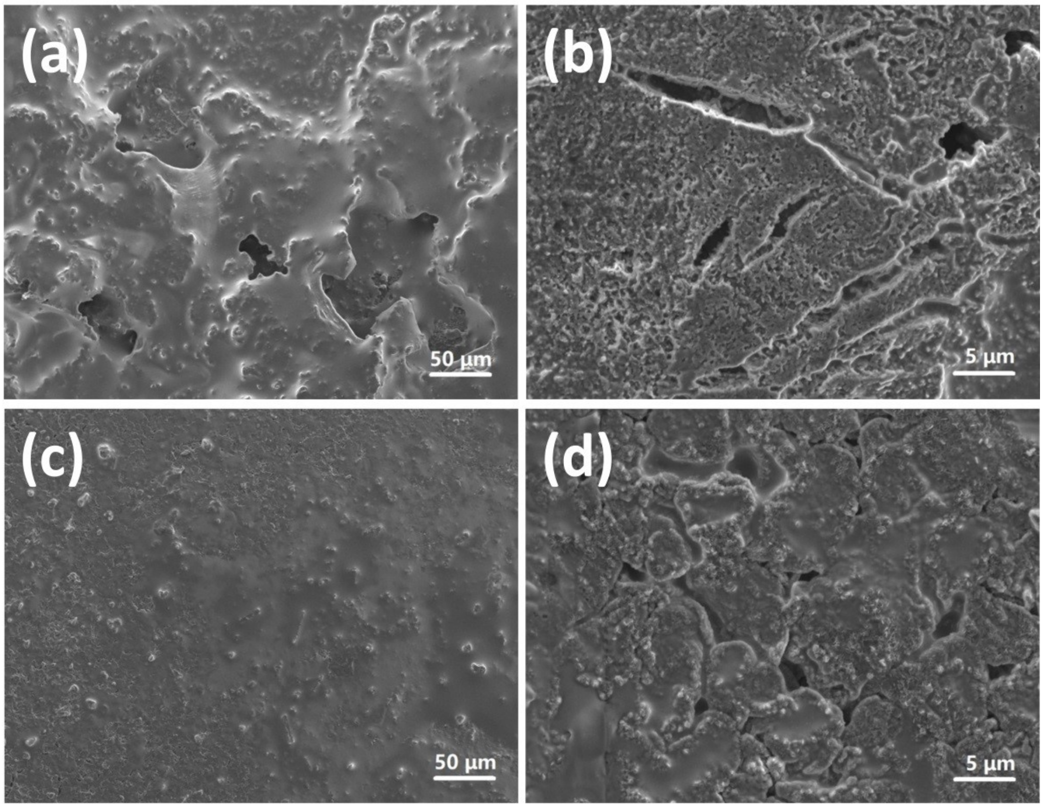


Figure S21. SEM images of Cu-Li//LFP (a,b) and MA-Zn-C-Li//LFP (c,d) at 0.44C after 200 cycles.

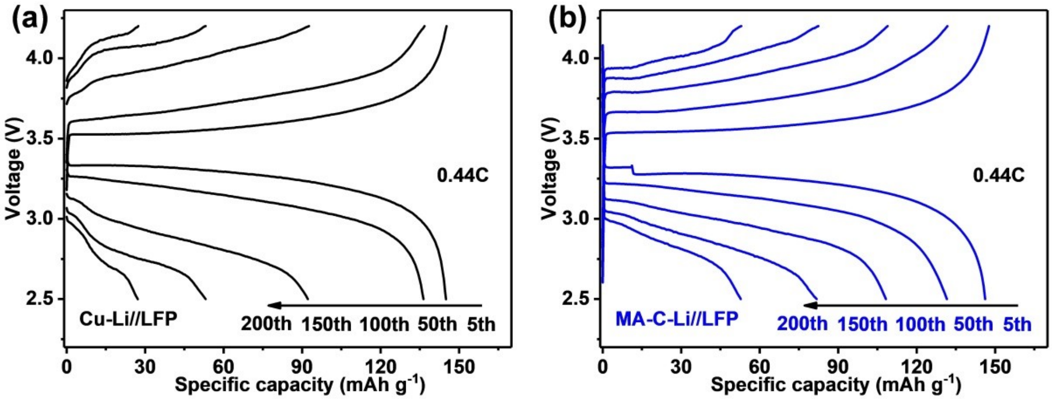


Figure S22. Charge/discharge curves of Cu-Li//LFP and MA-C-Li//LFP at 0.44C.

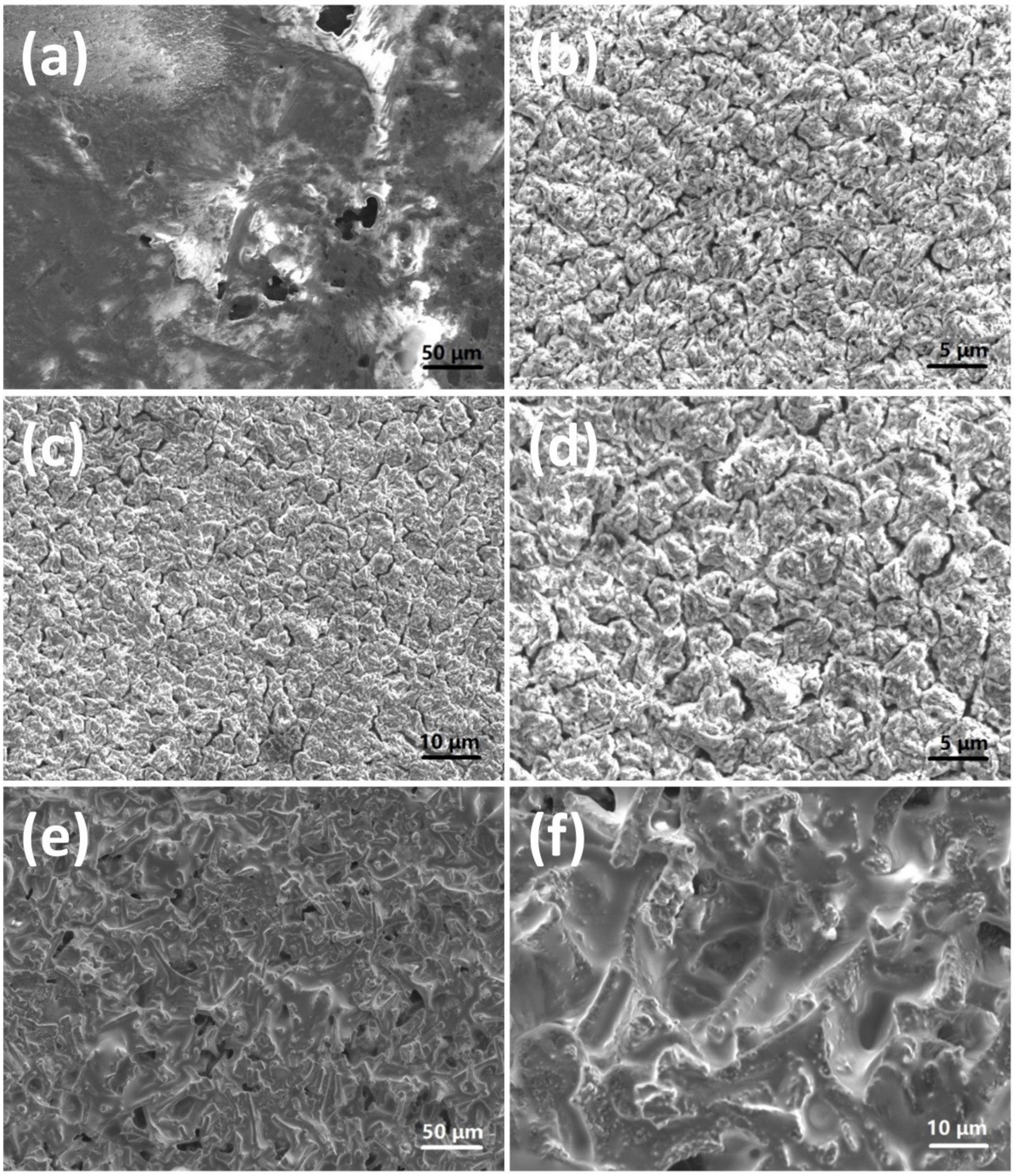


Figure S23. SEM images of Cu-Li//LFP (a,b), MA-C-Li//LFP (c,d) and MA-Zn-C-Li//LFP (e,f) at 1.77C after 500 cycles.

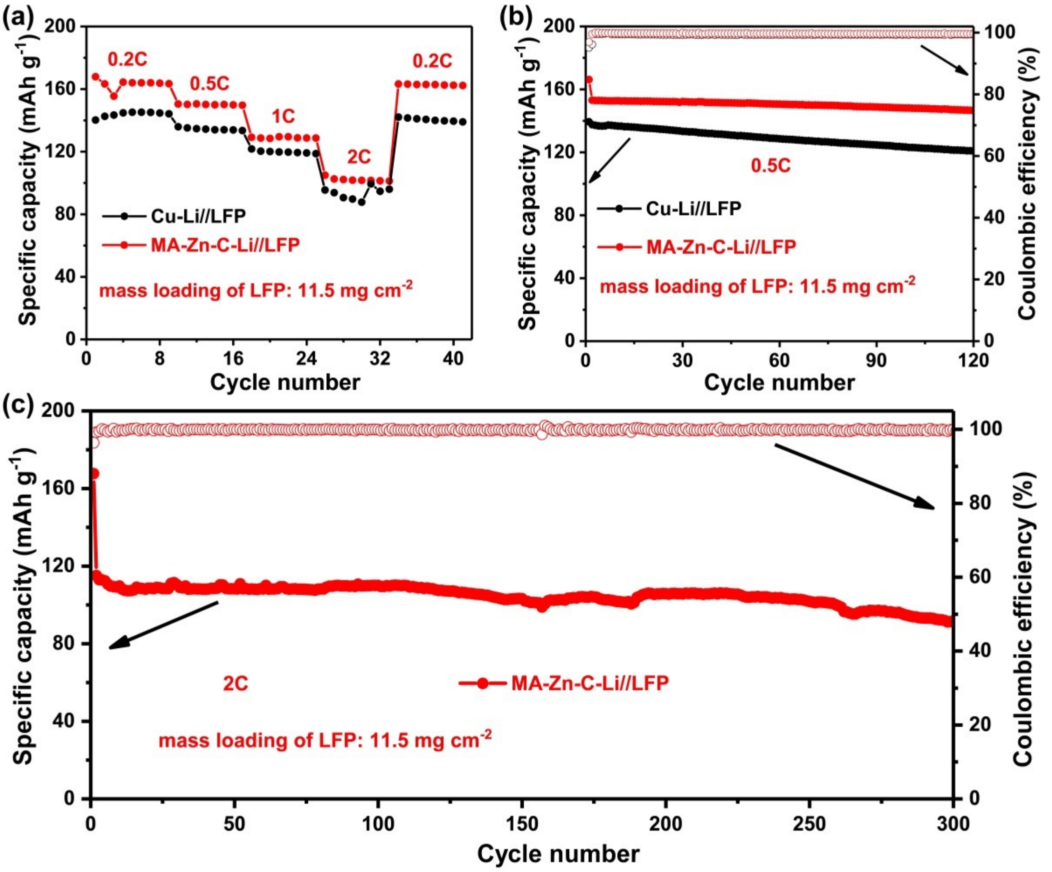


Figure S24. Electrochemical performances of full cells with Cu-Li or MA-Zn-C-Li anodes and LFP cathodes (mass loading: 11.5 mg cm$^{-2}$). (a) Rate capacity of Cu-Li//LFP and MA-Zn-C-Li//LFP. (b) Cycling stability of Cu-Li//LFP and MA-Zn-C-Li//LFP at 0.5C. (c) Cycling stability of MA-Zn-C-Li//LFP at 2C.

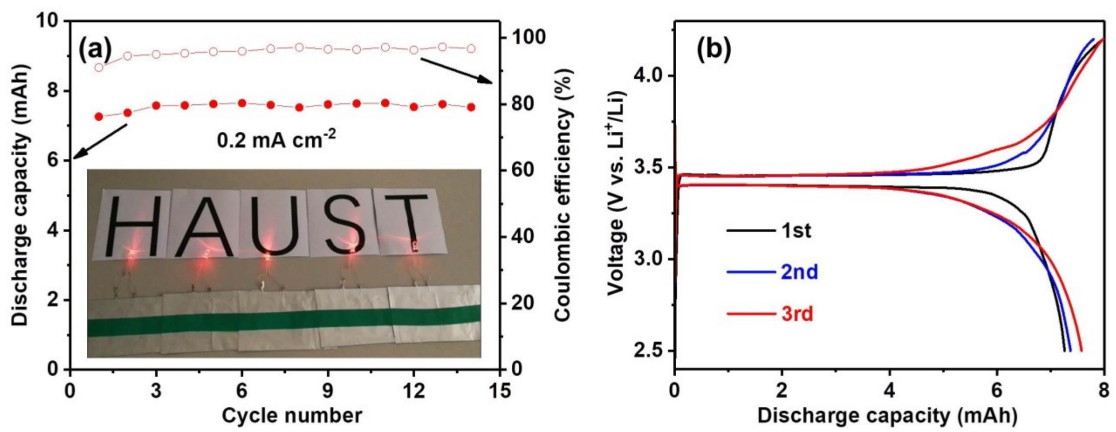


Figure S25. Electrochemical performances. (a) cycling performance of MA-Zn-C-Li//LFP pouch cells and (b) corresponding voltage profile.

Table S1. A survey of Li-based anodes with different carbon hosts and corresponding electrochemical properties with ether-based electrolyte.

| **Anode** | **Current Density (mA $cm^{-2}$)** | **Capacity (mAh $cm^{-2}$)** | **Overpotential (mV)** | **Cycle Life (h)** | **Refer.** |
|---|---|---|---|---|---|
| MA-Zn-C | 1 | 1 | 14 | 1200 | This work |
| | 5 | 5 | 16 | 1500 | |
| | 15 | 15 | ~82 | 500 | |
| C-400 | 1 | 1 | ~20 | 200 | [1] |
| CP/Sn/$SnO_2$ | 1 | 1 | 16 | 800 | [2] |
| | 2 | 1 | 16 | 250 | |
| FO-GCNs | 2 | 1 | ~25 | 800 | [3] |
| CHEMP@Ni | 5 | 2 | ~25 | 1370 | [4] |
| ACrCFs | 1 | 1 | ~15 | 1000 | [5] |
| NOCA@CF | 1 | 0.5 | ~14 | 800 | [6] |
| | 10 | 10 | ~185 | 400 | |
| NHCF/CN/ZnO | 1 | 1 | 25 | 1032 | [7] |
| | 2 | 1 | 25 | 1032 | |
| MCNFs/Ag | 1 | 1 | 20 | 600 | [8] |
| Co@NPC | 10 | 1 | 31 | 200 | [9] |

**C-400**:carbon cloth derived from cotton at 400 °C
**CP**：carbon paper
**FO-GCNs**：functionalized onion-like graphitic carbon nanospheres
**CHEMP@Ni**：nickel particles embedded in the holes of carbonized natural porous structure (hemp)
**ACrCFs**:carbon nanofibers decorated with uniform $CrO_{0.78}N_{0.48}$ nanoparticles
**NOCA@CF**: N/O dual doped 3D porous carbon architectures are designed on commercial Cu foam current collector
**NHCF/CN/ZnO**: Nitrogendoped hollow carbon fiber/carbon nanosheets/ZnO
**MCNFs/Ag**: 3D multichannel carbon fibers (MCNFs) that are decorated with lithiophilic Ag nanoparticles
**Co@NPC:** 3D carbon nanotubes and a N-doped carbon polyhedron core (PC) embedded with lithiophilic Co nanoparticles

References:
(1) J. K. Meng, W. W. Wang, X. Y. Yue, H. Y. Xia, Q. C. Wang, X. X. Wang, Z. W. Fu, X. J. Wu and Y. N. Zhou, *Journal of Power Sources*, 2020, **465**.
(2) L. Tan, S. H. Feng, X. H. Li, Z. X. Wang, W. J. Peng, T. C. Liu, G. C. Yan, L. J. Li, F. X. Wu and J. X. Wang, *Chemical Engineering Journal*, 2020, **394**.
(3) S. Ha, J. C. Hyun, J. H. Kwak, H. D. Lim and Y. S. Yun, *Small*, 2020, **16**.
(4) P. F. Wang, Z. Gong, K. Ye, Y. Y. Gao, K. Zhu, J. Yan, G. L. Wang and D. X. Cao, *Electrochimica Acta*, 2020, **356**.
(5) J. Xiao, N. Xiao, C. Liu, H. Q. Li, X. Pan, X. Y. Zhang, J. P. Bai, Z. Guo, X. Q. Ma and J. S. Qiu, *Small*, 2020, **16**.
(6) Y. L. An, Y. Tian, Y. Li, C. L. Wei, Y. Tao, Y. P. Liu, B. J. Xi, S. L. Xiong, J. K. Feng and Y. T. Qian, *Chemical Engineering Journal*, 2020, **400**.
(7) X. L. Zhang, Z. Q. Ruan, Q. T. He, X. J. Hong, X. Song, Q. F. Zheng, J. H. Nie, Y. P. Cai and H. X. Wang, *Acs Applied Materials & Interfaces*, 2021, **13**, 3078-3088.
(8) L. Yu; Q. Su; B. Li; W. Liu; M. Zhang; S. Ding; G. Du; B. Xu. *Electrochimica Acta* **2020,** *362*.
(9) R. Jiang; W. Diao; D. Xie; F. Tao; X. Wu; H. Sun; W. Li; J. Zhang. *ACS Applied Energy Materials* **2021,** *4* (11), 12871-12881.